Emerging Superionic Sulfide and Halide Glass-Ceramic Solid Electrolytes: Recent Progress and Future Perspectives

Jingui Yang, Jing Lin, Torsten Brezesinski, and Florian Strauss*

Institute of Nanotechnology (INT), Karlsruhe Institute of Technology (KIT), Kaiserstr. 12, 76131 Karlsruhe, Germany.
*Corresponding author: florian.strauss@kit.edu

Abstract

Solid-state batteries (SSBs) are attracting attention as safe, high energy- and power density electrochemical energy-storage systems. However, they are not yet capable of outperforming advanced lithium-ion batteries using liquid electrolytes. A critical obstacle relates to the development of cost-effective, inorganic solid electrolytes (SEs), combining superionic conductivity with high (electro)chemical stability and mechanical softness. Realizing intrinsically soft, inorganic SEs is particularly challenging. Glass-ceramic SEs offer several advantages, but typically exhibit low ionic conductivities. Given the recent developments of sulfide- and halide-based glass-ceramic materials, the overall objective of designing superionic (inorganic) SEs, entailing polymer- or clay-like softness, seems feasible. These SEs benefit from lower processing temperatures and versatile chemistries that allow for further enhancements. This Review provides a comprehensive overview of recent developments in the field of lithium glass-ceramic SEs and maps out factors governing conductivity and mechanical behavior. Finally, opportunities, challenges, and design principles for next-generation SEs are discussed.

The increasing demand for safe, reliable, and affordable energy-storage devices for portable electronics, electric vehicles, and stationary energy storage has triggered extensive research and development in the last decades.[1] Conventional lithium-ion batteries (LIBs) using organic liquid electrolytes (LEs) are currently state-of-the-art with respect to energy and power density; however, they are about to approach their physicochemical limits. Solid-state batteries (SSBs) possibly enabling the application of high-capacity anodes (e.g., Li metal or silicon) and fast charging rates, along with improved safety, are considered as promising alternatives. However, before their

commercialization, several hurdles mainly related to interface instabilities and scalable fabrication need to be overcome.[2–4] In principle, SSBs rely on a solid electrolyte (SE) which acts as both separator between anode and cathode and as catholyte. This poses several chemical and mechanical requirements to such materials to ensure stable battery performance.[5–7] First, they need to be highly Li-ion conducting with a target value over 10 mS cm^{-1} at room temperature to enable good performance at high current rates.[8] Second, they need to be (electro)chemically stable or form stable interfaces in contact with the active electrode materials. Third, they must exhibit appropriate mechanical properties to accommodate volume and morphology changes of the active electrode materials during charge/discharge and avoid Li dendrite penetration.[9–13]

The main type of SEs currently under investigations are polymer-, oxide-, and sulfide-based Li-ion conducting materials. Each of these material classes presents several advantages and disadvantages referring to the above-mentioned requirements.[14–18] For example, polymer-based SEs possess favorable mechanical properties, i.e., they are soft and allow establishing intimate contact with the active electrode materials and are additionally easy to implement in current roll-to-roll processing technologies used for LIB fabrication. Yet, their rather low ionic conductivities (~10^{-4} mS cm^{-1}) do not allow them to be operated at room or low temperatures. Besides, their poor oxidative stability poses additional challenges to long-term cell operation. Nevertheless, polymer-based cells with $LiFePO_4$ (LFP) cathode and Li-metal anode operating at 60 °C have been commercialized in the past.[19,20]

Hybrid or composite SEs, for instance, consisting of a polymer and an oxide-based material, have been investigated too. However, they suffer from rather low ionic conductivities and stability issues.[21–24] In contrast, oxide-based Li-ion conducting ceramics possess a high electrochemical stability, allowing combining high-voltage cathodes with a Li-metal anode. However, they possess moderate room-temperature ionic conductivities (~1 mS cm^{-1}), are very brittle, and need to be sintered at high temperatures to minimize grain-boundary resistances and reduce porosity. For that reason, they are difficult to be integrated into SSB cells.[25–28] Sulfide-based SEs would be much more favorable, as they are soft (low Young's modulus), can achieve very high ionic conductivities even if cold pressed, and allow for intimate contact with the active electrode materials. A few examples of sulfide- or thiophosphate-based Li-ion conductors have been demonstrated in the past with ionic conductivities similar or even

higher than LEs, rendering them ideal SEs at first sight. Unfortunately, their (electro)chemical stability window is very narrow, and therefore, protective (buffer) layers need to be applied to the cathode active material (CAM) as well as to the anode to avoid severe (electro)chemical degradation.[17,29,30] Generally speaking, it seems challenging to meet all requirements in one material, thus the quest for advanced SEs is ongoing. In this line, halide SEs have recently attracted great attention, as they offer a high oxidative stability, paired with a relatively low hardness, and can achieve reasonably high ionic conductivities.[31–37]

All of the above-discussed SEs, except for polymers, are typically well-crystallized materials. This has been thought to be a necessity for achieving high ionic conductivities. However, from a chemo-mechanical point of view, glassy or glass-ceramic SEs consisting of amorphous or mixed amorphous-nanocrystalline phases would be much more favorable, as they are much softer, need lower processing temperatures, possess a greater resistance to Li dendrite formation, and have a diverse chemistry.[38,39] Various oxide-, sulfide-, and halide-based glassy or glass-ceramic SEs have been reported throughout the last decades, with ionic conductivities often being too low for application in bulk-type SSBs (unlike crystalline SEs).[38,40] This paradigm has been overcome given recent developments of highly conducting, sulfide- and halide-based glassy or glass-ceramic SEs. This research opens up new opportunities in the development for advanced SEs providing advantages with regards to electrochemical stability, mechanical softness, combined with high ionic conductivities. In the following, we give a brief overview of state-of-the-art materials, summarize factors governing their ionic conductivity and soft mechanical properties, and finally discuss opportunities and challenges for the development of advanced glass-ceramic SEs.

Recent Developments of Superionic Glass-Ceramic Solid Electrolytes

In the following paragraph, we outline recently developed superionic sulfide- and halide-based glass-ceramic SEs. We divide the section into different classes of materials based on their anion chemistry, referring to halide and chalcohalide materials, in addition to sulfide and thiophosphate/borohydride SEs. An overview of measured/reported conductivities is given in **Table S1** (Supporting Information).

Sulfide-based glass-ceramic SEs are widely studied, among them the $70Li_2S–30P_2S_5$ system received most attention, as ionic conductivities, comparable to those of liquid

electrolytes, could be achieved.[38,41] The high ionic conductivity within this system can be assigned to the formation of highly conducting $Li_7P_3S_{11}$ nanoparticles, crystallizing from the amorphous precursor blend around 250 °C.[41–43] However, this phase possesses a poor thermal stability and decomposes to other less conductive lithium thiophosphates above 280 °C.[42] Due to this relatively narrow stability window, and therefore, difficulties in controlling crystallization and grain-boundary structure, the reported ionic conductivities of $Li_7P_3S_{11}$-based glass-ceramic SEs vary a lot in the literature.[41,44] The highest total conductivity achieved is $1.7 \cdot 10^{-2}$ S cm^{-1} (from melt quenching and subsequent hot pressing), while the lowest is $2.7 \cdot 10^{-4}$ S cm^{-1} (from solution synthesis).[45,46] Nevertheless, conductivities around 3 mS cm^{-1} seem to be regularly achievable.[41,47] The crystallization process and grain boundaries within the glass-ceramic Li_2S–P_2S_5 system could also be tailored by slightly varying the Li_2S-to-P_2S_5 molar ratio in the synthesis and introducing additives. Liquan *et al.* recently used Al_2S_3, SiS_2, or Ga_2S_3 as nucleation accelerant in the $72Li_2S$–$28P_2S_5$ system.[48] After heating at 300 °C, the presence of different nanocrystalline phases ($Li_7P_3S_{11}$, Li_3PS_4, $Li_{2.85}Al_{0.05}PS_4$) was observed. The unique phase composition of the as-synthesized composite caused the formation of highly conducting grain-boundary regions, leading to ionic conductivities of up to $1.3 \cdot 10^{-2}$ S cm^{-1}. There are only few other reported sulfide-based glass-ceramic SEs with ionic conductivities well above 1 mS cm^{-1}. The first example has been reported based on the Li_2S−P_2S_5−LiI system.[49] Starting from amorphous $0.33LiI$–$0.67Li_3PS_4$ prepared by ball milling, the conductivity could be drastically increased from 0.8 to 6.5 mS cm^{-1} by heating at 180 °C for 30 min.[49,50] The annealing temperature was set to be 10 °C lower than the crystallization temperature determined from differential scanning calorimetry (DSC) measurements; X-ray diffraction (XRD) showed no obvious differences before and after the heat treatment.[49,50] For the $x Li_3PS_4$–$y LiBH_4$ system, ionic conductivities above 6 mS cm^{-1} have been reported, where a complex mixture of amorphous and nanocrystalline phases has been detected, with various P–S polyhedral units being present.[51,52] This contrasts with recent research on halide and chalcohalide glass-ceramic or glassy SEs. As indicated in **Table S1**, several examples of materials exhibiting 10 mS cm^{-1} have been reported by now. Different combinations of glass formers ($TaCl_5$, $AlCl_3$, GaF_3, etc.) and binary Li salt additives (LiF, LiCl, LiBr, LiI, etc.) were proven to be able to form amorphous SEs via high-energy ball milling of the respective precursors. This research has been initiated by the report of Ju-Sik *et al.*, reporting a clay-like 2LiCl–

GaF_3 amorphous SE with a room-temperature ionic conductivity of $3.6 \cdot 10^{-3}$ S cm^{-1} in 2021.[53] They demonstrated its applicability, where the soft-mechanical properties allowed filling the SE into pores of the conventional slurry-cast cathode sheet under pressure (at room temperature). However, due to the poor reductive stability of this SE, it could only serve as catholyte. The highest conductivity of such halide-based glass-ceramic SEs was realized by Long *et al.*, who were using the $2LiCl–55AlF_3–45GaF_3$ system and achieved $1.6 \cdot 10^{-2}$ S cm^{-1} at room temperature. However, SSB performance has not been reported.[54] In the aforementioned examples of halide-based glass-ceramic SEs, solely GeF_3 has been used as a glass former in combination with lithium halide salts. Meanwhile similarly high Li-ion conducting halide-based glass ceramics have been demonstrated, employing $TaCl_5$, $NbCl_5$, or $HfCl_4$ as glass formers.[54–58] For example, Yasuo *et al.* systematically studied the $LiX–TaCl_5$ glass-ceramic SEs with X = F, Cl, Br, I, finding that $LiCl–TaCl_5$ and $LiF–TaCl_5$ can achieve both high ionic conductivity and good oxidative stability.[55] Several of these SEs were employed in SSBs, together with $LiNi_{0.91}Co_{0.06}Mn_{0.03}O_2$ cathodes, and showed high Coulomb efficiencies (CEs) and excellent cycling stability, though the amorphous SEs also only served as catholytes to avoid reduction in contact with the InLi anode. Apart from using lithium halide additives, Li_2O has been studied as network modifier, together with $TaCl_5$ and $HfCl_4$, by Zhang and colleagues among others, and few oxyhalide-based SEs have been reported up to now.[56,56,59,60] By compositional optimization, $1.6Li_2O–TaCl_5$ and $1.5Li_2O–HfCl_4$ glass-ceramic SEs achieved high ionic conductivities of $6.6 \cdot 10^{-3}$ S cm^{-1} and $1.97 \cdot 10^{-3}$ S cm^{-1}, respectively, and their performance as catholytes was demonstrated in SSBs.[56]

To put the above-mentioned recent developments of highly conducting sulfide and halide amorphous-nanocrystalline SEs into context, the range of ionic conductivities given in **Table S1** is schematically depicted in **Figure 1a**. In principle, the reported highly conducting glass-ceramic SEs can be grouped into four different classes related to the anion chemistry, i.e., halide, halide/chalcogenide, sulfide and thiophosphate/borohydride. A liquid electrolyte with a partial ionic conductivity of 2.7 mS cm^{-1} is represented in the form of a dashed-dotted line for reference. Note that SEs require a much higher ionic conductivity than liquid electrolytes, primarily due to more tortuous transport pathways in the electrodes. Unlike in liquid electrolyte-based systems, where the electrolyte can properly wet the surface of active material, in SSBs, the (interfacial) contact area between the SE and the active material is much smaller

(the electrode preparation strongly relies on mechanical mixing). In addition, the inevitable void space present in SSB electrodes, formed either during preparation or cell cycling because of detrimental chemo-mechanical processes, further exacerbates this issue. This makes it challenging to form efficient charge transport paths for fully exploiting the material's intrinsic ionic conductivity. Therefore, a target ionic conductivity of at least 10 mS cm^{-1} has been suggested for SSBs with practical active mass loadings and reasonable charging rates.[8,61] Ionic conductivities exceeding 10 mS cm^{-1} have been reported only for halide- and sulfide-based glass ceramic SEs, which has been established as a threshold value enabling fast-charging SSBs.[4,8]

A meta-analysis for the different classes of SEs reveals generalizable trends, as depicted in **Figure 1b**, illustrated in the form of a box-and-whisker plot. In general, it can be seen that the median ionic conductivity increases in the following order: halides < chalcohalides < sulfides < thiophosphate/borohydrides. The exceptionally high values reported for $2LiCl–0.5AlF_3–0.5GaF_3$ and $54Li_2S–21P_2S_5–3Al_2S_3$ can be considered as outliners, and future work will show if such conductivities can be realized with other compositions as well.[48,54] Nevertheless, the best-performing examples of all four material classes are able to achieve ionic conductivities well above 2.7 mS cm^{-1}. Considering the low number of reported compositions, they present a versatile starting ground for further optimization of conductivity, electrochemical stability, and mechanical softness.

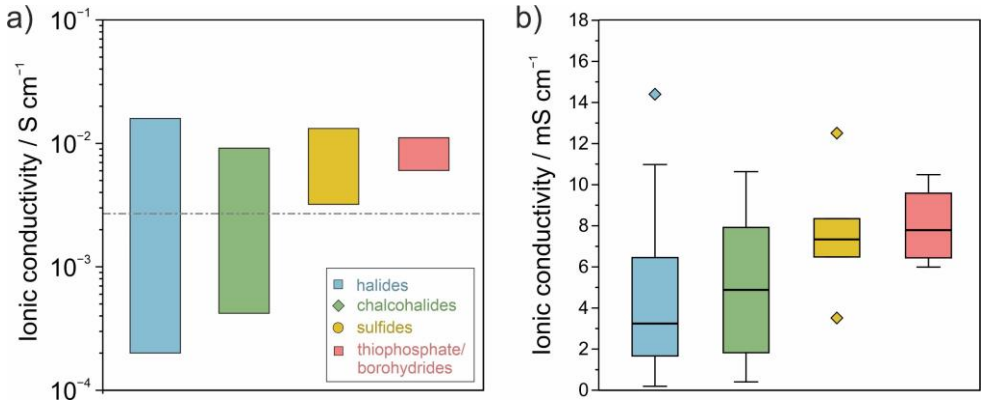

Figure 1. (a) Reported room-temperature ionic conductivity ranges for highly conducting halide-, chalcohalide-, sulfide-, and thiophosphate/borohydride-based glass-ceramic SEs as given in **Table S1**. The partial ionic conductivity of 1 M $LiPF_6$ in EC/DMC is shown for comparison as a gray dashed-dotted line.[8,61] (b) Corresponding box-and-whisker plot of the ionic conductivities. For halides, chalcohalides, sulfides, and thiophosphate/borohydrides, *n* = 30, 14, 5, and 4, respectively.

Factors Governing Superionic Conductivity and Soft-Mechanical Behavior

Classical theories for crystalline SEs usually take the polyhedral network as a static framework and the charge carriers hop among available lattice sites, so the crystal structure and the charge-carrier and vacancy concentrations together govern the ionic conduction. However, recent studies indicate that the rotational dynamics of polyanions, known as paddle-wheel mechanism or recently introduced soft-cradle effect,[62] may increase cation diffusivity, thereby enhancing ionic conductivity.[63,64] The paddle-wheel and soft-cradle effects, while not exclusive to amorphous SEs, are indeed more pronounced in amorphous SEs than in their crystalline counterparts, especially at room temperature. The paddle-wheel effect involves large-angle rotation of anion groups, whereas the soft-cradle effect is associated with the tilting of polyanions triggered by ion jumps.[62] In crystalline SEs with weaker van der Waals forces between the polyhedral anions, like Li_6PS_5Cl and $Li_{10}GeP_2S_{12}$, the $[PS_4]^{3-}$ or $[GeS_4]^{4-}$ structural units exhibit a reorientation, as indicated by high-temperature *ab initio* molecular dynamics (AIMD) simulations or ^{31}P nuclear magnetic relaxation studies.[64] However, these polyhedral rotations and reorientations are more prominent in amorphous SEs, likely due to the lower degree of structural confinement and increased free volume. In glass-ceramic or glassy Li-ion conductors, different mechanisms, leading to superionic conduction, can be at play, depending on the elemental and phase compositions.

In the following, we discuss recent examples showing high ionic conductivities in either sulfide- or halide-based glass-ceramic Li-ion conductors. Although ion conduction in chalcogenide glasses is well known for decades, a major improvement in ionic conductivity has only recently been achieved. This refers to the $x\mathrm{Li_2S}$–$y\mathrm{P_2S_5}$–$z\mathrm{M_aS_b}$ and $0.33\mathrm{LiI}$–$0.67\mathrm{Li_3PS_4}$ material systems. In the former case, Li_2S and P_2S_5 are combined in ratios closely matching the $Li_7P_3S_{11}$ phase, and are partially substituted with Al_2S_3, Ga_2S_3, or SiS_2. Ionic conductivities well beyond 5 mS cm^{-1} were achieved after heating the amorphous precursor mixture at 300 °C for 8 h.[48] In the case of Al_2S_3 substitution, both $Li_7P_3S_{11}$ and $Li_{2.82}Al_{0.06}PS_4$ form, accompanied with a ~5 nm amorphous grain boundary network connecting the crystallites. In the grain-boundary regions, ions are redistributed due to the difference in chemical potential of the two nanocrystalline phases, and therefore, a defect-rich region is formed, enabling fast ion conduction reaching 13.2 mS cm^{-1} (see **Figure 2a**). This material is among the best-

conducting crystalline thiophosphates, and the approach possibly presents a novel route to make glass-ceramic SEs competitive with state-of-the-art (crystalline) SEs. In this regard, Masahiro *et al.* studied the crystallization behavior of the $75Li_2S–25P_2S_5$ glass via *in situ* transmission electron microscopy (TEM).[65] They found that heating below the crystallization temperature determined by DSC already triggers the formation of $Li_7P_3S_{11}$ nanocrystals, which remain invisible via examination with laboratory XRD. This example emphasizes that even low contents of secondary phases may have a profound impact on ionic conductivity, in line with reports about mixed thiophosphate/borohydride materials. Another intriguing example is the recently reported material that can be obtained if an amorphous mixture of $1.5Li_2S–0.5P_2S_5–0.33LiI$ (i.e., $0.33LiI–0.67Li_3PS_4$) is subjected to heating at 180 °C for 30 min. Through this procedure, the ionic conductivity could be increased from around 0.8 to 6.5 mS cm^{-1}.[49,50] It is shown that this annealing step causes the formation of a mixture of Li_4PS_4I, *β*-Li_3PS_4, and a thio-lithium superionic conductor (thio-LISICON) II phase (see **Figure 2b**). Thio-LISICON II phases refer to materials with a similar structure to $Li_{3.25}Ge_{0.25}P_{0.75}S_4$.[66] Although the mechanism behind the high ionic conductivity in the $0.33LiI–0.67Li_3PS_4$ system is yet not fully understood, it can be assumed that in addition to the thio-LISICON II phase being responsible for the increase in conductivity, the presence of a nanocrystalline and highly disordered Li_4PS_4I phase is also beneficial to ion transport, in agreement with recent work.[67–69] The authors reported that the short heat treatment introduces vacancies in the amorphous phase(s), causing the increased ionic conductivity.[49,70] Although glass-ceramic electrolytes lack long-range ordering, stable Li sites exist in the amorphous matrix. Despite challenges in identifying and describing these sites experimentally, MD simulations revealed that in glassy (i.e., amorphous) SEs, the number of available sites surpasses the number of lithium atoms. This enables the ions to hop between vacant sites, thereby forming a conductive network.[71] In the short-term annealed $0.33LiI–0.67Li_3PS_4$ system, the authors found, by ^7Li nuclear magnetic resonance (NMR) spectroscopy, that heating improves ion transport in the amorphous phase. Positron-annihilation lifetime (PLA) analysis showed a 2.8-fold increase in vacancy concentration, suggesting that the presence of lithium vacancies is beneficial to the ionic conductivity.[49] However, their formation mechanism remains largely unclear, and further investigations into the local structural evolution during annealing are required to explain the increased number of lithium-site vacancies. Overall, the results open up new avenues for the improvement of glass-

ceramic SEs regarding ionic conductivity, which has been a major obstacle for their practical application.

Similar to the sulfide SEs, combinations of thiophosphate and borohydride materials have been shown to also achieve high ionic conductivities. Specifically, the presence of a complex mixture of amorphous and nanocrystalline phases has been detected, along with various P–S polyhedral units. It can be concluded that achieving very high ionic conductivities in fully amorphous sulfide- or thiophosphate-based SEs seems not feasible and a certain amount of nanocrystalline phases embedded in the amorphous matrix is necessary. However, due to the lack of systematic investigations into highly conducting glass-ceramic SEs, targeted synthesis of specific phase compositions remains challenging.

Transitioning from sulfide- to halide-based glass-ceramic SE materials, it has been reported that in gallium-containing chalcogenide glasses, adding halides increases the glass-forming ability. For example, introducing binary alkali metal chlorides into the GeS_2–Ga_2S_3 system produces complex polyanions of GaS_3Cl/GaS_2Cl, facilitating glass formation.[72] This agrees with observations that increasing CsI contents in the GeS_2–In_2S_3 system causes a decrease in glass-transition temperature, and a softening point below room temperature has been demonstrated for the GaI–NaCl system.[72,73] Various metal halides have also been introduced into other chalcohalide- or fluoride-based amorphous materials to improve the glass-forming ability and lower the glass.-transition temperature, which has been hypothesized to originate from the formation of complex polyanions.[74,75]

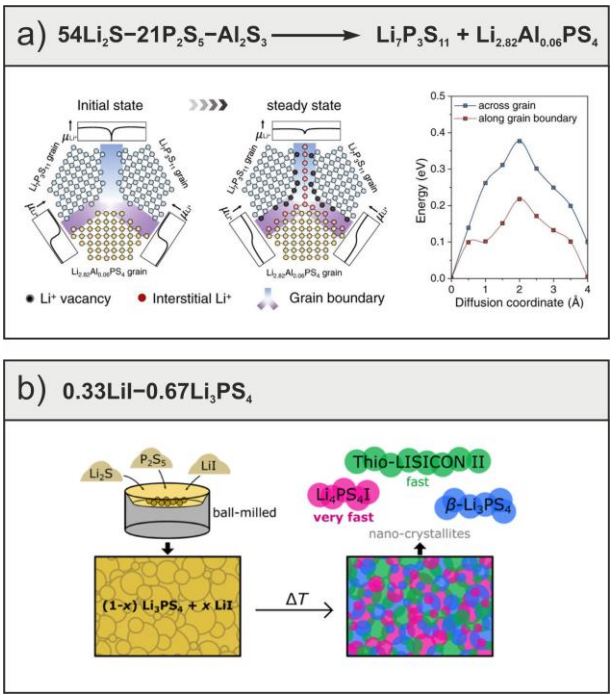

Figure 2. Thiophosphate-based glass-ceramic SEs based on (a) $Li_7P_3S_{11}$ and (b) Li_3PS_4. Corresponding ionic conductivities are given in **Table S1**. The figures have been adopted and reproduced with permission from ref. [48], Copyright 2023 Springer Nature, and reproduced with permission from ref. [50], Copyright 2021 American Chemical Society.

The presence of complex polyanionic environments also seems to be a key feature in halide-based glass-ceramic SEs possessing clay-like mechanical softness. In the following, four recently reported archetype materials are described. Initially, it has been shown that if LiCl and GaF_3 are combined in appropriate ratios and subjected to high-energy ball milling, a mostly glass-ceramic, clay-like material is formed, with ionic conductivities of up to 3 mS cm^{-1} achieved for the specific $2LiCl{-}GaF_3$ composition.[53] Using MD simulations and solid-state NMR spectroscopy, it has been found that if LiCl and GaF_3 are processed via ball milling, a partial anion exchange reaction is induced, leading to the formation of mixed $[GaF_xCl_y]^{[(x+y)-3]-}$ polyhedral units, as schematically shown in **Figure 3a**.[53,76,77] It was concluded that the presence of fluorine in the polyanions limits the binding effect on charge carriers, thus facilitating ion diffusion through the amorphous matrix.[76] Moreover, the formation of a complex polyanionic composition comes along with the amorphization and formation of a soft clay-like material, which is beneficial for SSB performance and integration. Gupta *et al.* recently investigated other potentially clay-forming compositions consisting of a molecular solid

and Li-halide, such as $3LiCl–SbF_3$, $3LiI–GaF_3$, or $3LiI–InBr_3$.[77] They revealed that complete anion exchange between the molecular solid and the Li-halide salt may occur upon high-energy milling and that the as-formed fully anion-exchanged products separate into macroscopic, crystalline phases (e.g., $3LiI + InBr_3 \rightarrow 3LiBr + InI_3$). By contrast, in the case of xLiCl–GaF_3, only partial anion exchange occurs, leading to the formation of different Ge polyhedral environments (see **Figure 3a**).[76] It has been hypothesized that the intrinsic bonding situation of GaF_3 kinetically impedes complete anion exchange and phase separation. Besides, the chemical bonding situation and ratios of the starting materials play important roles, too. In the halide-based materials mentioned above, isolated polyhedra are present and most likely responsible for amorphization, softening, and enhanced ionic conductivity. Such materials deviate from the classical understanding of the formation of a glass, where usually a 3-dimensional polyhedral network is formed via covalent bonding.

This brings us to the next example of a novel inorganic halide-based SE, which is the oxygen-substituted $LiAlCl_{2.5}O_{0.75}$.[58] This material shows a viscoelasticity comparable to that of polymers, along with an ionic conductivity of 1.52 mS cm^{-1}. The amorphization is enabled by oxygen substitution in $LiAlCl_4$, causing structural disorder through the formation of connected Al-tetrahedra via bridging O atoms (see **Figure 3b**). However, there is no long-range connectivity. Again, in this case, the appropriate ratio of O-to-Cl ensures a proper length of the Al–O–Al network, while the remaining free $[AlCl_x]^{3-x}$ units that are not connected by oxygen also act as plasticizer, both of which helps to lower the glass-transition temperature to −16.8 °C.[58] The authors revealed that the presence of Al–O–Al chains also promotes Li-ion conduction via shortening the hopping distance and motion of the Al–O–Al chains themselves. Note that the atomistic (local) structure and ion conduction mechanism in amorphous $LiAlCl_{2.5}O_{0.75}$ have been rationalized based on MD simulations, as experimental characterization of local structures and related transport processes is very challenging.

Recently, another oxygen-substituted halide-based amorphous SE has been reported, namely $x$$Li_2O$–$MCl_y$ with M = Ta (y = 5) or Hf (y = 4) reaching 6.6 mS cm^{-1} for x = 1.6 and M = Ta.[56] As described previously for other material systems, to achieve amorphization, the appropriate ratio of Li_2O-to-MCl_5 is necessary, lying in the narrow compositional range of $1.1 \leq x \leq 1.8$ for $TaCl_5$ and x = 1.5 for $HfCl_4$. If Li_2O is reacted with $TaCl_5$ via ball milling, the original Ta_2Cl_{10} dimers dissociate to -$TaCl_5$ trigonal bipyramids and further undergo anion-exchange reactions with oxygen forming

$[TaCl_{5-a}O_a]^{a-}$ polyhedra (see **Figure 3c**). Here, oxygen can also act as bridging atom connecting the Ta-centered trigonal bipyramids.[56] Specifically for x = 1.6, the most distorted polyhedral environment is formed. Based on this structural information, Zhang *et al.* concluded that the high ionic conductivity of $xLi_2O–TaCl_5$ amorphous SEs can be rationalized as follows: The oxygen-substituted disordered $[TaCl_{5-a}O_a]^{a-}$ ($1 \leq a \leq 5$) polyhedra cause distorted Li–Cl local arrangements. Moreover, the $[TaCl_{5-a}O_a]^{a-}$ polyhedra connected via bridging oxygen lead to the formation of corner-sharing polyhedral networks (similar to $LiAlCl_{2.5}O_{0.75}$), which induce distinct distortions in the Li sites, thereby causing an energy landscape with low ion migration energy. At the same time, the bridging oxygen atoms enlarge diffusion pathways for lithium, in agreement with observations made for other oxygen-substituted halide- and sulfide-based glasses.[58,78] In addition, the unsaturated Ta–Cl···Li bonds in the $[TaCl_{5-a}O_a]^{a-}$ network have weak Coulomb interactions between Li^+ and Cl^-, also facilitating ion diffusion. In short, oxygen incorporation is beneficial to the amorphization of $xLi_2O–TaCl_5$ and $LiAlCl_{2.5}O_{0.75}$, being responsible for their soft-elastic properties and inducing disordered local structures, which in turn leads to a strong increase in ionic conductivity and a decrease in activation energy compared to the single-anion $3.2LiCl–TaCl_5$ sample. However, if the LiCl-to-$TaCl_5$ molar ratio is set to 1:1 ($LiCl–TaCl_5$), ionic conductivities ranging between 6.05 and 10.95 mS cm^{-1} have been reported.[55,57] Theoretical and experimental analyses suggest that the amorphous matrix is composed of $LiCl_4^{3-}$, $LiCl_5^{4-}$, and $LiCl_6^{5-}$ polyhedra, in combination with $TaCl_6^-$ octahedra sharing common edges or corners (see **Figure 3d**). The number of neighboring Cl atoms around lithium ranges between four and six, whereas the number of Cl atoms around Ta does not vary, with only $TaCl_6^-$ octahedra existing within the amorphous matrix. If the LiCl content is increased to $x > 1$ in $xLiCl–TaCl_5$, full amorphization is not achieved anymore, and the presence of nanocrystalline LiCl is observed, adversely affecting the total ionic conductivity.[55] A similar local polyhedral environment around Ta has been reported for related Na- and Mg-ion conducting glass ceramics in the $0.5Na_2O_2–TaCl_5$ [79] and $xMgCl_2–GaF_3$ ($0.5 \leq x \leq 1.5$) [80] systems, emphasizing the versatile chemistry that can be used in the development of post-Li SEs.

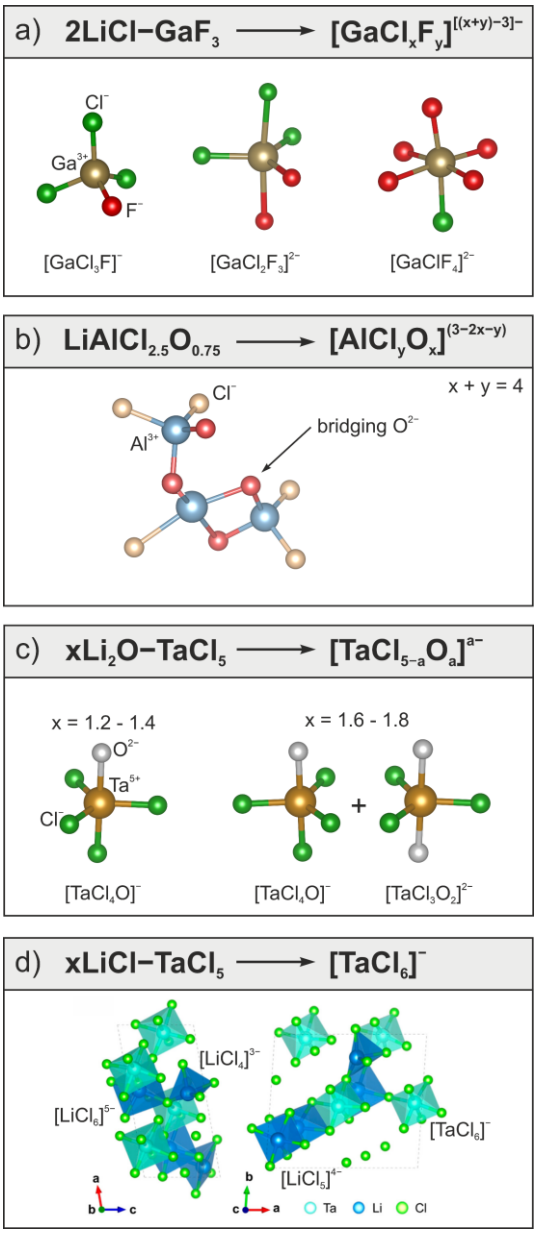

Figure 3. Polyhedral environments reported for (a) 2LiCl–GaF_3, (b) $LiAlCl_{2.5}O_{0.75}$, (c) LiCl–$TaCl_5$, and (d) *x*Li_2O–$TaCl_5$ glass-ceramic SEs. Ionic conductivities are given in **Table S1**. The structures in panel (d) have been adopted and reproduced with permission from ref. [55], Copyright 2023 American Chemical Society.

To sum up, different structural features that are responsible for superionic conductivity and mechanical softness in newly developed sulfide- and halide-based glass-ceramic SEs have been identified by now. Although various (ion-conducting) related materials are known for decades, pushing the ionic conductivity beyond 5 mS cm^{-1} is very challenging, and has only recently been realized. In the case of sulfide or thiophosphate materials, very high ionic conductivities have been achieved by tailoring the phase composition. Typically, amorphization of the precursor mixture is realized by

high-energy ball milling, followed by some kind of post treatment via annealing. The heating profile plays an important role, as it induces, at least to some degree, nucleation and crystallization, which in turn determines phase composition, crystallite size, and ultimately composition and structure of the amorphous side phase(s).[48–50] The physiochemical interplay of the different phases, especially at the grain boundaries, seems to be the major reason for facile ion transport. This is likely related to the well-established concept of space-charge layers and associated fast transport in nano-confined systems.[81] The complex microstructure and phase composition also account for the inherent softness of the discussed sulfide-based materials. However, rational improvement of ionic conductivity in sulfide-based glass ceramics remains challenging, as no global descriptors for superionic conductivity are apparent.

However, in the case of halide-based amorphous SEs, different mechanisms are at play, being responsible for high ionic conductivity and polymer-like softness and viscoelasticity. So far, all of these types of SEs are based on GaF_3, $TaCl_5$, $NbCl_5$, or $HfCl_4$, being the integral component responsible for amorphization and superionic conductivity. Charge carriers are introduced via mixing the aforementioned precursors with different binary Li salts, such as halides or oxides. In principle, these transition- or semi-metal precursors can be regarded as molecular solids (except GaF_3), in which dimers or linear polymers (e.g., Ta_2Cl_{10} or $[HfCl_4]_x$) are present, forming the crystal structure exclusively via van der Waals interactions (see **Figure 4**). Inorganic, molecular crystals usually have low melting points and are mechanical soft due to weak intermolecular interactions. Moreover, they are able to undergo anion-exchange reactions with binary Li salts, which can be achieved by high-energy ball milling. Such reactions can also be regarded as partial solid-state metathesis reactions and are likely facilitated and largely dependent on the bonding situation in the binary metal salt used. For example, the P–S bonds in P_4S_{10} have a strong covalent character compared to Nb_2Cl_{10}, and therefore, anion exchange seems more favorable in the latter case. At first sight, anion exchange might be explained using the HSAB-concept. However, reaction kinetics likely plays an important role, as in most reported cases, exchange has been achieved via low-temperature mechanochemistry.

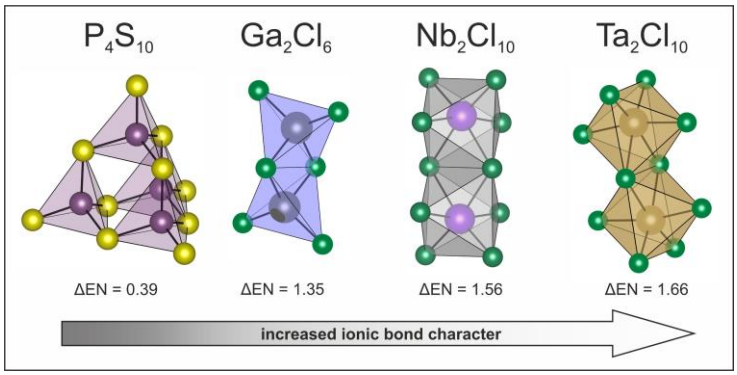

Figure 4. Basic building units of molecular crystals with the stoichiometry indicated. ΔEN refers to the difference in Pauling electronegativity of the different constituents and represents a simplified measure of the bonding situation.

Opportunities for Development of Sulfide and Halide Glass-Ceramic Solid Electrolytes

The recent reports about highly conducting sulfide- and halide-based glass-ceramic SEs represent a promising starting point for further explorations. Especially their favorable mechanical properties, in combination with superionic conductivity, render this class of materials very promising for SSB applications. Although only a limited number of material systems has been reported up to now, the general characteristics of glass-ceramic SEs in offering a much larger compositional, structural, and synthetic design space opens up vast possibilities for exploration and tailoring properties (in contrast to crystalline SEs). More importantly, they also possess much more favorable mechanical properties, i.e., softness, and are even able to form clay-like materials with viscoelastic properties similar to organic polymers, as evident for recently developed halide-based glass-ceramic SEs. This translates into easy processing and integration into SSB fabrication. Although the development of this kind of SEs is still in its infancy, the advantages over crystalline materials provide new opportunities in the realm of developing high-energy SSBs.

In the following section, we outline potential advantages and opportunities in the development of glass-ceramic SEs referring to ionic conductivity, mechanical properties, scalable synthesis, and the importance of controlling reaction pathways.

Vast Compositional Space

Since amorphous-nanocrystalline or glass-ceramic materials are not limited in terms of stoichiometry, they provide a practically infinite compositional (and structural) space.

This is likely advantageous if several material properties need to be tailored simultaneously, e.g., (electro)chemical and mechanical properties (for SSB application).

To obtain an amorphous material (i.e., glass), typically a glass former is needed. In the case of chalcogenide-type amorphous SEs, the glass former is usually a polyanionic material possessing a covalently bonded basic building unit (e.g., SiO_4^{4-}, PO_4^{3-}, PS_4^{3-}, BO_3^{3-}, etc.) able to produce condensed molecular species (e.g., $P_2O_7^{4-}$, $B_2O_5^{4-}$, $P_2S_6^{4-}$, $(SiO_2)_x$, etc.) or chains. Therefore, cross-linked 2- or 3-dimensional networks without long-range order can be formed during melting, being preserved at room temperature via fast cooling. Similarly, halide-based glasses are well known, however exhibiting a more ionic bonding character within the glass former (see also **Figure 4**) and not being prone to 2- or 3-dimensional network formation (rather, 1D polymer-like chains).[82] To tailor different functionalities of amorphous materials, a network modifier may be incorporated into the amorphous matrix, also called glass former. This is usually a binary inorganic salt (e.g., Li_2S, Li-halide, etc.), which not only is able to introduce mobile cation species, but also is able to modify the bonding situation and network of the glass former. In short, an increased content of network modifier will disturb the macromolecular, amorphous structure, thus leading to the presence of isolated basic building units. Consequently, the molar ratio of glass former-to-network modifier determines, to some extent, the molecular (short-range) structure of amorphous materials. For example, in the $x Li_2S–P_2S_5$ system, the main local thiophosphate units evolve from chain- $(PS_3^-)_n$ to corner-sharing (referring to $P_2S_7^{4-}$) to isolated PS_4^{3-} tetrahedra, triggered by an increase in Li_2S content x from 1 to 2 to 3. Finally, an additive crystalline phase(s) can be introduced into the amorphous material, either via partial crystallization or integrating a secondary phase(s). Again, depending on the amount and chemical nature of the additive salt, the local atomic structure of the amorphous matrix is altered, and grain boundaries differing from the bulk composition can be formed.

Aside from tailoring functionalities in glass-ceramic SEs by altering composition in terms of ratio between glass former, network modifier, and additive, the synthesis parameters also have a profound effect on the resulting properties. In principle, three distinct parameters can be identified for glass-ceramic SEs, namely the amorphization technique, the temperature profile, and the applied pressure during synthesis. Usually, crystalline precursors are employed, and the first step involves amorphization of the

blend. This can either be done by high-energy milling (i.e., mechanochemical synthesis), melt quenching, or solution-based methods. Each technique has its own advantages and disadvantages with respect to processing time, energy consumption, and scalability. Amorphization by milling is most often time and energy consuming and further limited to gram-scale batches, thus limiting practicality for upscaling. Melt-quenching, industrially well established, is a rather fast process, however requiring more costly equipment, especially if air-sensitive glasses are to be produced. Solution- or solvent-based methods offers advantages in terms of scalability, but solvent removal needs to be considered, too. This synthesis technique offers opportunities to controlling the product particle size by adjusting parameters, such as the nature of solvents, concentration of additives, or reaction time. For example, nucleophilic solvents, such as acetonitrile (ACN), tetrahydrofuran (THF), and pyridine, or nucleophilic reagents (e.g., lithium thioethoxide) are commonly used to break the covalent bonds of the P_4S_{10} precursor and to obtain an amorphous product.[83,84] However, strong interactions between solvent and precursors might pose a significant challenge to fully removing the solvent from the product. That is why SEs prepared by solution-based methods often exhibit lower ionic conductivities than those obtained by solvent-free synthesis routes. While there have been no reports on wet-chemical syntheses of halide-based glass-ceramic electrolytes, crystalline halide SEs have been successfully produced using a water-based approach.[85] For example, LiCl and $InCl_3$ precursors readily dissolve into water to form $Li_3InCl_6{\cdot}xH_2O$, which upon drying at 200 °C under vacuum yields Li_3InCl_6 of ionic conductivity 2 mS cm^{-1}. Recently, NH_4Cl has been introduced as a coordinating agent to suppress undesired hydrolysis reactions of chlorides, thereby extending the solution synthesis to other halide SEs.[86] These findings indicate the potential for preparing halide-based glass-ceramic electrolytes via solution-based routes, yet further experiments are required to substantiate this possibility.

Independent of the technique applied, successful amorphization of the precursor mixture is generally confirmed by laboratory XRD, with the corresponding patterns being featureless. Nevertheless, some differences in short-range ordering are likely present on the atomic scale, which may also have an impact on the global material properties (see also discussion below).[87] Once an amorphous material is obtained, its nano- and microstructure can be altered by heating at different temperatures for different periods of times and under external pressure. DSC is a common analytical

tool used to examine glass transition-, crystallization-, and melting temperatures. Specifically, temperatures of interest can be identified, and then targeted in the post-treatment to induce crystallization of a secondary phase. The latter is embedded in an amorphous matrix in the form of nanoscale precipitates, whose average size can be tailored through the dwell time, which directly affects the ionic conductivity, either positively or negatively.[48–50,69] The formation of nanocrystalline precipitates from the amorphous starting material(s) is strongly dependent upon the heating procedure, i.e., heating and cooling rates and dwelling time.[49] Although the crystallization of nanoscale precipitates has been reported to strongly increase conductivity, their detection via laboratory XRD is challenging and more sophisticated analytical techniques are required to gain more insights.[48,49] In addition, beneficial or detrimental effects on ionic conductivity are hard to be predicted, since during heating multiple phases may start to crystallize. As mentioned above, DSC can provide valuable insights into glass transition-, crystallization, and melting temperatures. However, in reality, such process is much more complex and involves also softening, nucleation, and crystal growth, all accompanied by volume changes. All of these individual processes can be detected *in situ* using a hot-press setup able to simultaneously monitor pressure and resistance by following a pre-defined temperature program.[42,67] In so doing, the optimum annealing temperature can be more precisely determined. Moreover, it has been reported that applying external pressure during heating can delay crystallization in the case of thiophosphate ion conductors.[67] Therefore, pressure is another important parameter in the synthesis of glass-ceramic SEs, not only affecting crystallization kinetics, but also helping to densify the sample and ultimately to increase ionic conductivity.[42,67]

Enabling Superionic Conductivity

Crystalline SEs present microscopic heterogeneity due to the anisotropic nature of crystals. For instance, ion transport within a crystal might be directionally preferred, with the presence of grain boundaries impeding long-range ion transport. Note that inhomogeneous ion transport can lead to increased cell resistance, potentially deteriorating the SSB performance. In addition, non-uniform current distributions can give rise to the formation of lithium dendrites. These dendritic structures pose a significant concern, as they can compromise the battery integrity, leading to safety problems, such as short circuits, and reduced cycle life. On the contrary, no preferential

ion diffusion pathways usually exist in amorphous, glass-ceramic SEs, and their low intrinsic electronic conductivities minimize local ion-current accumulation, which might be beneficial to uniform Li plating/stripping in SSBs.[88] Despite decades of research into Li-ion conducting glass-ceramics, only recently ionic conductivities comparable to those of crystalline SEs and liquid electrolytes have been reported. These studies provide clear evidence that achieving ionic conductivities above 10 mS cm^{-1} is feasible with sulfide- and halide-based systems.[48,54] In the case of sulfide-based glass-ceramics, the unique interplay of different amorphous and nanocrystalline phases primarily accounts for the high ionic conductivities.[48–50] In particular, the formation of Li-rich grain-boundary regions, favorable to fast ion transport, appears to be the enabler for superionic conductivity.[48] Enhanced ion transport along space-charge layers is well known,[89,90] however very high ionic conductivities in bulk samples have only recently been realized. Therefore, both *in situ* formation of multiphase, amorphous-nanocrystalline SEs and artificially mixing different amorphous and nanocrystalline phases to induce bulk superionic conductivity are promising strategies for developing future sulfide-based SEs. By contrast, halide-based glass-ceramic SEs do not rely on conductivity contributions from grain boundaries and/or nanocrystalline phases. Rather, the highly distorted local environment around the Li-ions in the amorphous matrix makes them highly mobile.[56,58] Therefore, in contrast to establishing favorable interactions between different amorphous and nanocrystalline phases, as described above for sulfide-based glass-ceramic SEs, local structural distortions seem to be key to improving ionic conductivity in halide-based materials. So far, all reported highly ion-conducting systems are based on molecular crystal precursors, where ligand (anion) exchange between the glass former and the network modifier occurs upon mechanical amorphization of the starting materials. Nevertheless, the presence of highly disordered local structural environments seems necessary to achieve competitive ionic conductivities.[54–56,58] In the end, this may relate to compositional complex or high-entropy materials, although per definition configurational entropies can only be determined from crystalline species with shared site occupancies.

Enabling Mechanical Softness

It is well established by now that mechanically soft SEs, i.e., with low elastic moduli, are beneficial for enhancing SSB performance, especially for mitigating capacity fading.[69,91–93] Glass-ceramic SEs typically exhibit lower elastic moduli compared to

crystalline counterparts.[10,94] This is due in part to the ability of glass-ceramic SEs to achieving improved surface wetting and to effectively accommodating electrode breathing during cycling, thus maintaining cell integrity.[93,95] To tailor mechanical properties in glassy (amorphous) SEs, a wide variety of elements can be introduced into the amorphous matrix, and the proportions of glass former, network modifier, and additive(s) can be varied with great flexibility. Additionally, the size and distribution of crystallites and residual porosity play a crucial role in the mechanical properties. The latter can be optimized by carefully controlling the synthesis conditions.[42,96] Furthermore, it is worth noting that the composition of the amorphous and nanocrystalline phases does not necessarily have to be identical. With precise control over crystallization conditions, nanocrystalline phases with different compositions from the amorphous matrix can be realized. This allows customizing the properties of both phases, offering the potential of achieving superior performance.

Another step toward polymer-like behavior of inorganic SEs has been taken recently for (oxy)halide-based systems. Here, a key point seems to be precise control over anion ratio, enabling the formation of flexible glass networks, while the weak intermolecular interactions in halide- or chalcohalide-based amorphous SEs (similar to molecular solids) make them intrinsically very soft.[77] This leads to some compositions having a rheology comparable to that of clay-like materials, and further allows the SEs to be infiltrated into slurry-cast cathodes by applying mild pressure and moderate temperatures, as schematically depicted in **Figure 5**.

Although not very well understood at this time, further exploration into anion-mixed, highly disordered systems could facilitate the development of glass-ceramic SEs that are capable of outperforming state-of-the-art liquid electrolytes for LIB application. From the recent examples of halide-based superionic glass-ceramics, it appears that they have high oxidative but rather poor reductive electrochemical stability. The latter is most likely related to the presence of transition or semimetal species (i.e., glass former), which can readily be reduced. Therefore, halide-based superionic SEs might be applicable only as catholytes, or ultimately as protective surface coatings on high-voltage CAMs. In contrast, sulfide-based glass ceramics have been reported to form stable interfaces in contact with lithium metal. However, they suffer from poor oxidative stability. Consequently, a dual-layer SSB design using both classes of glass-ceramic SEs appears to be promising for future investigations. In such a design, in addition to the (electro)chemical stability, the chemical compatibility between the two SEs is of

great importance and must be considered. For example, Li_6PS_5Cl and Li_3InCl_6 dual-layer SSB configurations have been found unstable, with a poorly conductive indium/sulfur-rich interfacial layer forming at the junction.[7,97] This reaction appears to be catalyzed by Ni-rich CAMs, even though the underlying mechanism is still unclear (of note, more reactions occur at the triple-phase boundary). One theory suggests that the chemical compatibility between halides and sulfides can be explained by the hard–soft acid–base (HSAB) principle.[98] Specifically, the greater the electronegativity of the central metal atoms in the halide SE, the more likely it is to form covalent bonds with sulfur atoms from the sulfide SE, which however can only partially explain the experimental findings. In this regard, it has been shown that Li_3InCl_6 and Li_2ZrCl_6 are unstable in contact with Li_6PS_5Cl, while Li_3YCl_6, Li_3ErCl_6, and Li_3ScCl_6 apparently exhibit reasonable stabilities.[99] Moreover, anion substitution in halide SEs seems to be an effective way to enhance their chemical stability against sulfide-based SEs.[100]

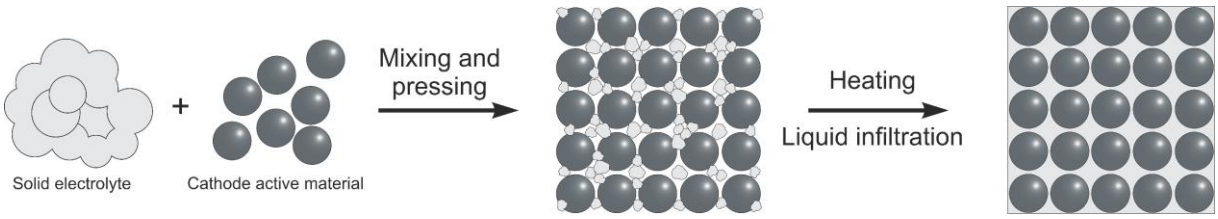

Figure 5. Schematic representation of electrode fabrication by melt infiltration. The figure is inspired from ref. [58]

Synthesis Upscaling and Solid-State Battery Applications

Glass-ceramic materials are commercially produced and used in various important applications. Therefore, upscaling should be feasible. However, their susceptibility to degradation under ambient atmosphere requires strict handling under inert conditions, possibly complicating production. Although, the synthesis does not require prolonged high-temperature sintering, thus saving time and energy (cost), they are almost exclusively prepared by high-energy milling (potentially followed by heating at relatively low temperatures). One important task of future investigations will be to find out whether similar performance metrics can be achieved if the materials are prepared by scalable synthesis protocols using melt-quenching or wet chemistry.

When it comes to commercial application and upscaling, another important parameter is raw material costs. With the globally rising demand for LIBs, the lithium (precursor) price becomes volatile.[101] Compared to liquid electrolytes, SEs typically exhibit a much

higher fraction of lithium, thus rendering them more costly.[2] It has been challenging so far to reduce the lithium content in SEs while maintaining superionic conductivity; yet, switching from sulfide- to chalcohalide- or halide-based glass-ceramic SEs seems promising. Especially the recently reported chalcohalide-based amorphous SEs, having a relatively low mass fraction of lithium. As can be seen from **Figure 6**, unlike sulfides, halide- and chalcohalide-based glass ceramics allow to drastically reduce the lithium fraction from about 10 to 2 wt.%. In addition to considering lithium content, some glass formers contain scarce metal species, such as Ge, Ta, Nb, and Hf, presenting significant cost challenges for large-scale application and thus might be more applicable as nanoscale CAM coatings. Therefore, it is essential to identify suitable, earth-abundant alternatives. For instance, the $LiAlCl_{2.5}O_{0.75}$ electrolyte, although only having a moderate ionic conductivity, contains no rare elements and has a relatively low lithium fraction of ~2 wt.%.[58] Apart from possible cost reductions, the mechanical flexibility of amorphous-nanocrystalline SEs and the potentially clay-like or viscoelastic behavior of halide-based SEs further help facilitate the fabrication process of SSBs, among others, by avoiding time- and energy-consuming wet mixing.

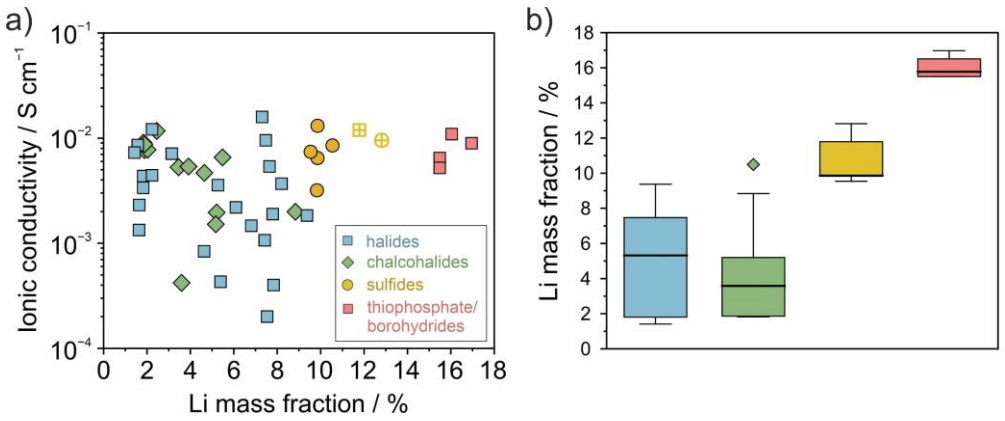

Figure 6. (a) Ionic conductivity of the glass-ceramic SEs given in **Table S1** versus the Li mass fraction. The square and circular reticle symbols in yellow denote crystalline $Li_{10}GeP_2S_{12}$ and $Li_{5.5}PS_{4.5}Cl_{0.7}Br_{0.8}$ for comparison.[102,103] (b) Corresponding box-and-whisker plot of the Li mass fractions. For halides, chalcohalides, sulfides, and thiophosphate/borohydrides, *n* = 30, 14, 5, and 4, respectively.

Controlling Reaction Pathways

Amorphous-nanocrystalline or glass ceramics can be considered metastable, with the corresponding thermodynamically stable form being a crystalline material. Therefore,

kinetic control over reaction pathways is most likely key to isolating metastable SEs with improved transport and mechanical properties. In classical glass formation, a melt is rapidly cooled to avoid nucleation and crystallization, thus the metastable, glassy product can be preserved at room temperature (see **Figure 7a**). The required cooling rate depends on the composition of each system, in particular on the diffusion kinetics (crystallization). As pointed out previously, in the case of sulfide-based SEs, complex (amorphous-nanocrystalline) compositions/phases and their interplay at grain boundaries determine the ion mobility. To achieve high conductivities, different synthesis parameters can be tuned. For example, adding nucleation agents may support the formation of crystalline, nanoscale precipitates from the amorphous matrix or setting the annealing temperature slightly below the crystallization temperature may induce subtle structural changes in the amorphous phase(s).[48–50] Additionally, external pressure applied during the heating may play a pivotal role in the phase formation (thermodynamics/kinetics) by increasing the activation energy for nucleation (see **Figure 7b**) or minimizing the reaction enthalpy, thereby opening up a new reaction pathways and enabling the stabilization of novel phase(s) (see **Figure 7c**).[67,104]

Halide-based amorphous-nanocrystalline or fully amorphous SEs are usually synthesized via amorphization of crystalline precursors during high-energy milling, i.e., GaF_3, $HfCl_4$, $NbCl_5$, or $TaCl_5$, together with binary lithium halides or chalcogenides. From a mechanistic point of view, this can be regarded a mechanochemical solid-state metathesis reaction, which can be simply expressed as: LiX + MY → MX + LiY. Such metathesis or double ion-exchange reactions are usually driven by the formation of a thermodynamically stable byproduct, along with the target material.[105] The combination of salt precursors (LiX and MY) must entail a thermodynamic driving force for anion exchange. However, the kinetics of the anion-exchange (metathesis) reaction must be slow enough or slowed down artificially to avoid complete anion exchange and phase separation. We assume that this is, at least to some degree, related to the dissociation energy of binary precursors, particularly the glass-forming metal halides. Further control is achieved by altering the precursor salt ratio, ensuring that neither of the compounds is present in much excess. If complete anion exchange occurs, the products macroscopically separate into crystalline phases, as observed by combining 3LiCl with SbF_3 or 3LiI with $InBr_3$.[77] Complete anion exchange, i.e., metathesis reaction, must be avoided when aiming at amorphous materials. This means that intermediate (metastable) products need to be stabilized (see **Figure 7a**). Overall,

kinetic control over the metathesis reaction is key to synthesizing novel halide-based amorphous SEs. We hypothesize that primarily the bonding situation in the transition/semimetal halide precursor and the ratio with the binary halide salt determine the reaction kinetics. Hence, controlling these parameters, along with the temperature, will eventually allow for kinetic control over the reaction pathway and for progress to be made in the synthetic development of superionic SEs. Another related synthesis strategy has been reported recently, where the byproduct was removed from the equilibrium to drive the reaction toward product formation. For instance, oxygen incorporation into $LiAlCl_4$ has been achieved via the following reaction: $4LiAlCl_4 + Sb_2O_3 \rightarrow 4LiAlCl_{2.5}O_{0.75} + 2SbCl_3$. The latter reaction was performed at 250 °C, which allowed for removing gaseous $SbCl_3$.[58] However, to rationally design such reactions, in-depth knowledge on the processes occurring on an atomistic level is indispensable.

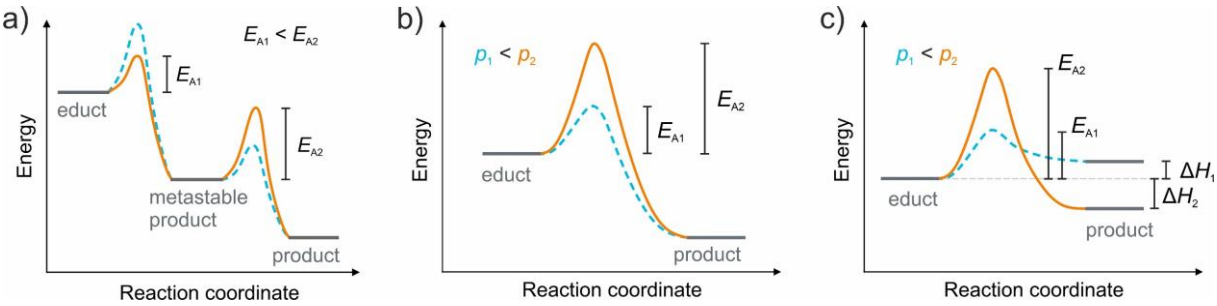

Figure 7. Schematic energy/reaction coordinate diagrams. (a) Kinetic control over reaction pathway enabling or preventing product formation, with the possibility of stabilizing (metastable) intermediates. (b, c) Reaction pathway control is achieved by changing pressure. The diagrams are inspired from refs. [67,104,105]

Guiding Principles for Future Developments and Applications

Sulfide-Based Systems – Grain Boundaries and Complex Multiphase Compositions

Nanoscale channels and facile percolation pathways for fast Li-ion transport have to be established via designing a complex phase composition involving amorphous and nanocrystalline phases. In an ideal case Li-ion mobility is fostered in grain boundary and bulk regions, however systematic investigations are needed to establish suitable compositional and synthetically descriptors allowing for rational improvements.

Halide-Based Systems – Distorting the Polyanionic Environment via Anion Exchange

For halide SEs, the formation of highly complex and locally distorted polyanionic environments in halide-based SEs is key, which can be realized by tailoring the anion-exchange reactions (between lithium salts and molecular crystal-like transition or semimetal species). This allows for fast ion transport and polymer- or clay-like softness in halide-based SEs and potentially for developing a broad range of low-cost (environmentally friendly) compositions.

Application in Solid-State Batteries – Separator, Catholyte, and Surface Coating

Recent examples point toward the possibility of achieving soft-mechanical properties only in the case of halide-based systems. However, the respective materials only exhibit high oxidative stability and are not stable in contact with low-potential anodes. Therefore, they are likely only suited as catholytes (or protective surface coatings at the positive electrode side[106]), where high mechanical flexibility is demanded to accommodate for cathode volume changes. In contrast, sulfide-based systems are able to form kinetically stable interfaces with Li metal, present a certain mechanical strength, and thus seem applicable as separator in SSBs for preventing dendrite formation/growth. Despite these progresses, the interfacial instability between sulfide- and halide-based SEs is often overlooked. While the current understanding is limited, preliminary studies suggest that careful selection of materials and doping strategies can enhance the chemical stability of interfaces between different kinds of SEs. However, previous research has primarily focused on crystalline electrolytes, leaving a significant gap in understanding the interfacial properties of glass-ceramic electrolytes. Moving forward, efforts in developing dual-layer SSBs should clearly address the material stability, not only with respect to the positive and negative electrodes, but also at the junction of the combined SEs.

Conclusions and Outlook

In summary, we have outlined recent developments of superionic halide- and sulfide-based glass-ceramic SEs for SSB application. In particular, we aimed at giving a brief overview of the compositional, structural, and synthetic design space for glass-ceramics, recent examples of highly conducting glass-ceramics, and factors governing superionic conductivity, among favorable mechanical properties. Finally, we described potential opportunities and challenges in the further research and development of advanced glass-ceramic SEs. Especially the newly discovered halide-based systems

may lead to a paradigm shift in the development of next-generation, bulk-type SSBs. They present unique examples of combining high ionic conductivities with mechanical softness, i.e., polymer-like viscoelasticity or clay-like behavior. Overall, this seems to be a promising approach, as this class of materials entails the possibility of combining the advantages from polymer and inorganic electrolytes.

We believe that our Review sets the scope for future design of superionic sulfide- and halide-based glass-ceramic SEs by providing guidelines for targeted material exploration. Opportunities for achieving significant advancements in performance are high given the vast number of compositional and structural possibilities, including the development of ion conductors for post-Li chemistries.

Supplementary Information

Supporting Information is available. Overview of ionic conductivities and Li mass fractions reported for different halide, chalcohalide, sulfide, and thiophosphate/borohydride glass-ceramic SEs.

Author Biographies

Jingui Yang received his B.Sc. and M.Sc. degrees from Nanjing University in 2014 and 2018, respectively. He is currently a PhD student in the group of Florian Strauss at the Institute of Nanotechnology, focusing on the development and tailoring of glass-ceramic thiophosphate electrolytes for application in solid-state lithium batteries.

Jing Lin received her B.Sc. from Beijing University of Chemical Technology in 2015 and her M.Sc. degree from Karlsruhe Institute of Technology in 2021. She is currently a PhD student in the group of Florian Strauss at the Institute of Nanotechnology, investigating high-entropy solid electrolytes for solid-state battery application.

Torsten Brezesinski is a chemist by training, earning his doctorate in physical chemistry from the Max Planck Institute of Colloids and Interfaces/University of Potsdam in 2005. He is laboratory manager of BELLA and group leader at the Institute of Nanotechnology. His work encompasses, among others, the study of battery materials for electrochemical energy storage.

Florian Strauss received his cotutelle PhD in 2016 under the supervision of Prof. Tarascon and Prof. Dominko. He is currently a group leader at the Institute of Nanotechnology, working on the exploration of novel compositionally complex ceramic electrolytes and investigations into chemomechanics in solid-state batteries.

Acknowledgements

F.S. and J.Y. are grateful to the German Federal Ministry of Education and Research (BMBF) for funding within the project MELLi (03XP0447). J.L. acknowledges the Fond der Chemischen Industrie (FCI) for financial support.

Competing Interest

The authors declare no competing financial interest.

References

(1) Dunn, B.; Kamath, H.; Tarascon, J.-M. Electrical Energy Storage for the Grid: A Battery of Choices. *Science* **2011**, *334*, 928–935.

(2) Janek, J.; Zeier, W. G. Challenges in Speeding up Solid-State Battery Development. *Nat. Energy* **2023**, *8*, 230–240.

(3) Janek, J.; Zeier, W. G. A Solid Future for Battery Development. *Nature Energy* **2016**, *1*, 16141.

(4) Schmaltz, T.; Hartmann, F.; Wicke, T.; Weymann, L.; Neef, C.; Janek, J. A Roadmap for Solid-State Batteries. *Adv. Energy Mater.* **2023**, *13*, 2301886.

(5) Ye, T.; Li, L.; Zhang, Y. Recent Progress in Solid Electrolytes for Energy Storage Devices. *Adv. Funct. Mater.* **2020**, *30*, 2000077.

(6) Banerjee, A.; Wang, X.; Fang, C.; Wu, E. A.; Meng, Y. S. Interfaces and Interphases in All-Solid-State Batteries with Inorganic Solid Electrolytes. *Chem. Rev.* **2020**, *120*, 6878–6933.

(7) Chen, R.; Li, Q.; Yu, X.; Chen, L.; Li, H. Approaching Practically Accessible Solid-State Batteries: Stability Issues Related to Solid Electrolytes and Interfaces. *Chem. Rev.* **2020**, *120*, 6820–6877.

(8) Bielefeld, A.; Weber, D. A.; Janek, J. Modeling Effective Ionic Conductivity and Binder Influence in Composite Cathodes for All-Solid-State Batteries. *ACS Appl. Mater. Interfaces* **2020**, *12*, 12821–12833.

(9) Koerver, R.; Aygün, I.; Leichtweiß, T.; Dietrich, C.; Zhang, W.; Binder, J. O.; Hartmann, P.; Zeier, W. G.; Janek, J. Capacity Fade in Solid-State Batteries: Interphase Formation and Chemomechanical Processes in Nickel-Rich Layered Oxide Cathodes and Lithium Thiophosphate Solid Electrolytes. *Chem. Mater.* **2017**, *29*, 5574–5582.

(10) Koerver, R.; Zhang, W.; de Biasi, L.; Schweidler, S.; Kondrakov, A. O.; Kolling, S.; Brezesinski, T.; Hartmann, P.; Zeier, W. G.; Janek, J. Chemo-Mechanical Expansion of Lithium Electrode Materials – On the Route to Mechanically Optimized All-Solid-State Batteries. *Energy Environ. Sci.* **2018**, *11*, 2142–2158.

(11) Doux, J.-M.; Yang, Y.; Tan, D. H.; Nguyen, H.; Wu, E. A.; Wang, X.; Banerjee, A.; Meng, Y. S. Pressure Effects on Sulfide Electrolytes for All Solid-State Batteries. *J. Mater. Chem. A* **2020**, *8*, 5049–5055.

(12) Zhang, W.; Schröder, D.; Arlt, T.; Manke, I.; Koerver, R.; Pinedo, R.; Weber, D. A.; Sann, J.; Zeier, W. G.; Janek, J. (Electro)Chemical Expansion during Cycling: Monitoring the Pressure Changes in Operating Solid-State Lithium Batteries. *J. Mater. Chem. A* **2017**, *5*, 9929–9936.

(13) Berckmans, G.; De Sutter, L.; Marinaro, M.; Smekens, J.; Jaguemont, J.; Wohlfahrt-Mehrens, M.; van Mierlo, J.; Omar N. Analysis of the effect of applying external mechanical pressure on next generation silicon alloy lithium-ion cells. Electrochim. Acta **2019**, *306*, 387–395

(14) Bachman, J. C.; Muy, S.; Grimaud, A.; Chang, H.-H.; Pour, N.; Lux, S. F.; Paschos, O.; Maglia, F.; Lupart, S.; Lamp, P.; Giordano, L.; Shao-Horn, Y. Inorganic Solid-State Electrolytes for Lithium Batteries: Mechanisms and Properties Governing Ion Conduction. *Chem. Rev.* **2016**, *116*, 140–162.

(15) Asano, T.; Sakai, A.; Ouchi, S.; Sakaida, M.; Miyazaki, A.; Hasegawa, S. Solid Halide Electrolytes with High Lithium-Ion Conductivity for Application in 4 V Class Bulk-Type All-Solid-State Batteries. *Adv. Mater.* **2018**, *30*, 1803075.

(16) Gao, Z.; Sun, H.; Fu, L.; Ye, F.; Zhang, Y.; Luo, W.; Huang, Y. Promises, Challenges, and Recent Progress of Inorganic Solid-State Electrolytes for All-Solid-State Lithium Batteries. *Adv. Mater.* **2018**, *30*, 1705702.

(17) Lau, J.; DeBlock, R. H.; Butts, D. M.; Ashby, D. S.; Choi, C. S.; Dunn, B. S. Sulfide Solid Electrolytes for Lithium Battery Applications. *Adv. Energy Mater.* **2018**, *8*, 1800933.

(18) Zhang, Z.; Shao, Y.; Lotsch, B.; Hu, Y.-S.; Li, H.; Janek, J.; Nazar, L. F.; Nan, C.-W.; Maier, J.; Armand, M. New Horizons for Inorganic Solid State Ion Conductors. *Energy Environ. Sci.* **2018**, *11*, 1945–1976.

(19) Agrawal, R. C.; Pandey, G. P. Solid Polymer Electrolytes: Materials Designing and All-Solid-State Battery Applications: An Overview. *J. Phys. D: Appl. Phys.* **2008**, *41*, 223001.

(20) Long, L.; Wang, S.; Xiao, M.; Meng, Y. Polymer Electrolytes for Lithium Polymer Batteries. *J. Mater. Chem. A* **2016**, *4*, 10038–10069.

(21) Zhang, Z.; Wang, X.; Li, X.; Zhao, J.; Liu, G.; Yu, W.; Dong, X.; Wang, J. Review on Composite Solid Electrolytes for Solid-State Lithium-Ion Batteries. *Mater. Today Sust.* **2023**, *21*, 100316.

(22) Dirican, M.; Yan, C.; Zhu, P.; Zhang, X. Composite Solid Electrolytes for All-Solid-State Lithium Batteries. *Materials Science and Engineering: R: Reports* **2019**, *136*, 27–46.

(23) Croce, F.; Appetecchi, G. B.; Persi, L.; Scrosati, B. Nanocomposite Polymer Electrolytes for Lithium Batteries. *Nature* **1998**, *394*, 456–458.

(24) Chen, X. C.; Liu, X.; Samuthira Pandian, A.; Lou, K.; Delnick, F. M.; Dudney, N. J. Determining and Minimizing Resistance for Ion Transport at the Polymer/Ceramic Electrolyte Interface. *ACS Energy Lett.* **2019**, *4*, 1080–1085.

(25) Zhao, G.; Suzuki, K.; Okumura, T.; Takeuchi, T.; Hirayama, M.; Kanno, R. Extending the Frontiers of Lithium-Ion Conducting Oxides: Development of Multicomponent Materials with γ-Li_3PO_4-Type Structures. *Chem. Mater.* **2022,** *34*, 3948–3959.

(26) Wei, R.; Chen, S.; Gao, T.; Liu, W. Challenges, Fabrications and Horizons of Oxide Solid Electrolytes for Solid-State Lithium Batteries. *Nano Select* **2021**, *2*, 2256–2274.

(27) Schreiber, A.; Rosen, M.; Waetzig, K.; Nikolowski, K.; Schiffmann, N.; Wiggers, H.; Küpers, M.; Fattakhova-Rohlfing, D.; Kuckshinrichs, W.; Guillon, O.; Finsterbusch, M. Oxide Ceramic Electrolytes for All-Solid-State Lithium Batteries – Cost-Cutting Cell Design and Environmental Impact. *Green Chem.* **2023**, *25*, 399–414.

(28) Jiang, P.; Du, G.; Cao, J.; Zhang, X.; Zou, C.; Liu, Y.; Lu, X. Solid-State Li Ion Batteries with Oxide Solid Electrolytes: Progress and Perspective. *Energy Technol.* **2023**, *11*, 2201288.

(29) Park, K. H.; Bai, Q.; Kim, D. H.; Oh, D. Y.; Zhu, Y.; Mo, Y.; Jung, Y. S. Design Strategies, Practical Considerations, and New Solution Processes of Sulfide Solid Electrolytes for All-Solid-State Batteries. *Adv. Energy Mater.* **2018**, *8*, 1800035.

(30) Reddy, M. V.; Julien, C. M.; Mauger, A.; Zaghib, K. Sulfide and Oxide Inorganic Solid Electrolytes for All-Solid-State Li Batteries: A Review. *Nanomaterials* **2020**, *10*, 1606.

(31) Nie, X.; Hu, J.; Li, C. Halide-Based Solid Electrolytes: The History, Progress, and Challenges. *Interdisciplinary Materials* **2023**, *2*, 365–389.

(32) Nikodimos, Y.; Su, W.-N.; Hwang, B. J. Halide Solid-State Electrolytes: Stability and Application for High Voltage All-Solid-State Li Batteries. *Adv. Energy Mater.* **2023**, *13*, 2202854.

(33) Tuo, K.; Sun, C.; Liu, S. Recent Progress in and Perspectives on Emerging Halide Superionic Conductors for All-Solid-State Batteries. *Electrochem. Energy Rev.* **2023**, *6*, 17.

(34) Liu, Z.; Ma, S.; Liu, J.; Xiong, S.; Ma, Y.; Chen, H. High Ionic Conductivity Achieved in $Li_3Y(Br_3Cl_3)$ Mixed Halide Solid Electrolyte via Promoted Diffusion Pathways and Enhanced Grain Boundary. *ACS Energy Lett.* **2021**, *6*, 298–304.

(35) Li, X.; Kim, J. T.; Luo, J.; Zhao, C.; Xu, Y.; Mei, T.; Li, R.; Liang, J.; Sun, X. Structural Regulation of Halide Superionic Conductors for All-Solid-State Lithium Batteries. *Nat. Commun.* **2024**, *15*, 53.

(36) Hennequart, B.; Platonova, M.; Chometon, R.; Marchandier, T.; Benedetto, A.; Quemin, E.; Dugas, R.; Lethien, C.; Tarascon, J.-M. Atmospheric-Pressure Operation of All-Solid-State Batteries Enabled by Halide Solid Electrolyte. *ACS Energy Lett.* **2024**, *9*, 454–460.

(37) Gao, X.; Liu, B.; Hu, B.; Ning, Z.; Jolly, D. S.; Zhang, S.; Perera, J.; Bu, J.; Liu, J.; Doerrer, C.; Darnbrough, E.; Armstrong, D.; Grant, P. S.; Bruce, P. G. Solid-State Lithium Battery Cathodes Operating at Low Pressures. *Joule* **2022**, *6*, 636–646. h

(38) Lin, L.; Guo, W.; Li, M.; Qing, J.; Cai, C.; Yi, P.; Deng, Q.; Chen, W. Progress and Perspective of Glass-Ceramic Solid-State Electrolytes for Lithium Batteries. *Materials* **2023**, *16*, 2655.

(39) Wheaton, J.; Olson, M.; Iii, V. M. T.; Martin, S. W. Glassy Solid-State Electrolytes for All-Solid- State Batteries. *American Ceramic Society Bulletin* **2023**, *102*, 24–31.

(40) Grady, Z. A.; Wilkinson, C. J.; Randall, C. A.; Mauro, J. C. Emerging Role of Non-Crystalline Electrolytes in Solid-State Battery Research. *Front. Energy Res.* **2020**, *8,* 218.

(41) Zhou, J.; Chen, P.; Wang, W.; Zhang, X. $Li_7P_3S_{11}$ Electrolyte for All-Solid-State Lithium-Ion Batteries: Structure, Synthesis, and Applications. *Chem. Eng. J.* **2022**, *446*, 137041.

(42) Busche, M. R.; Weber, D. A.; Schneider, Y.; Dietrich, C.; Wenzel, S.; Leichtweiss, T.; Schröder, D.; Zhang, W.; Weigand, H.; Walter, D.; Sedlmaier, S. J.; Houtarde, D.; Nazar, L. F.; Janek, J. *In Situ* Monitoring of Fast Li-Ion Conductor $Li_7P_3S_{11}$ Crystallization Inside a Hot-Press Setup. *Chem. Mater.* **2016**, *28*, 6152–6165.

(43) Yamane, H.; Shibata, M.; Shimane, Y.; Junke, T.; Seino, Y.; Adams, S.; Minami, K.; Hayashi, A.; Tatsumisago, M. Crystal Structure of a Superionic Conductor, $Li_7P_3S_{11}$. *Solid State Ionics* **2007**, *178*, 1163–1167.

(44) Chu, I.-H.; Nguyen, H.; Hy, S.; Lin, Y.-C.; Wang, Z.; Xu, Z.; Deng, Z.; Meng, Y. S.; Ong, S. P. Insights into the Performance Limits of the $Li_7P_3S_{11}$ Superionic Conductor: A Combined First-Principles and Experimental Study. *ACS Appl. Mater. Interfaces* **2016**, *8*, 7843–7853.

(45) Ito, S.; Nakakita, M.; Aihara, Y.; Uehara, T.; Machida, N. A Synthesis of Crystalline $Li_7P_3S_{11}$ Solid Electrolyte from 1,2-Dimethoxyethane Solvent. *J. of Power Sources* **2014**, *271*, 342–345.

(46) Seino, Y.; Ota, T.; Takada, K.; Hayashi, A.; Tatsumisago, M. A Sulphide Lithium Super Ion Conductor Is Superior to Liquid Ion Conductors for Use in Rechargeable Batteries. *Energy Environ. Sci.* **2014**, *7*, 627–631.

(47) Mizuno, F.; Hayashi, A.; Tadanaga, K.; Tatsumisago, M. New Lithium-Ion Conducting Crystal Obtained by Crystallization of the Li_2S–P_2S_5 Glasses. *Electrochem. Solid-State Lett.*, **2005**, *8*, A603–A606.

(48) Wang, Y.; Qu, H.; Liu, B.; Li, X.; Ju, J.; Li, J.; Zhang, S.; Ma, J.; Li, C.; Hu, Z.; Chang, C.-K.; Sheu, H.-S.; Cui, L.; Jiang, F.; van Eck, E. R. H.; Kentgens, A. P. M.; Cui, G.; Chen, L. Self-Organized Hetero-Nanodomains Actuating Super Li+ Conduction in Glass Ceramics. *Nat. Commun.* **2023**, *14*, 669.

(49) Spannenberger, S.; Miß, V.; Klotz, E.; Kettner, J.; Cronau, M.; Ramanayagam, A.; di Capua, F.; Elsayed, M.; Krause-Rehberg, R.; Vogel, M.; Roling, B. Annealing-Induced Vacancy Formation Enables Extraordinarily High Li^+ Ion Conductivity in

the Amorphous Electrolyte 0.33LiI + 0.67Li_3PS_4. *Solid State Ionics* **2019**, *341*, 115040.

(50) Miß, V.; Neuberger, S.; Winter, E.; Weiershäuser, J. O.; Gerken, D.; Xu, Y.; Krüger, S.; di Capua, F.; Vogel, M.; Schmedt auf der Günne, J.; Roling, B. Heat Treatment-Induced Conductivity Enhancement in Sulfide-Based Solid Electrolytes: What Is the Role of the Thio-LISICON II Phase and of Other Nanoscale Phases? *Chem. Mater.* **2022**, *34*, 7721–7729.

(51) Jang, Y.-J.; Seo, H.; Lee, Y.-S.; Kang, S.; Cho, W.; Cho, Y. W.; Kim, J.-H. Lithium Superionic Conduction in BH4-Substituted Thiophosphate Solid Electrolytes. *Adv. Sci.* **2023**, *10*, 2204942.

(52) Wang, D.; Jhang, L.-J.; Kou, R.; Liao, M.; Zheng, S.; Jiang, H.; Shi, P.; Li, G.-X.; Meng, K.; Wang, D. Realizing High-Capacity All-Solid-State Lithium-Sulfur Batteries Using a Low-Density Inorganic Solid-State Electrolyte. *Nat. Commun.* **2023**, *14*, 1895.

(53) Jung, S.-K.; Gwon, H.; Yoon, G.; Miara, L. J.; Lacivita, V.; Kim, J.-S. Pliable Lithium Superionic Conductor for All-Solid-State Batteries. *ACS Energy Lett.* **2021**, *6*, 2006–2015.

(54) Xu, R.; Yao, J.; Zhang, Z.; Li, L.; Wang, Z.; Song, D.; Yan, X.; Yu, C.; Zhang L. Room Temperature Halide-Eutectic Solid Electrolytes with Viscous Feature and Ultrahigh Ionic Conductivity. *Adv. Sci.* **2022**, *9*, 2204633.

(55) Li, F.; Cheng, X.; Lu, G.; Yin, Y.-C.; Wu, Y.-C.; Pan, R.; Luo, J.-D.; Huang, F.; Feng, L.-Z.; Lu, L.-L.; Ma, T.; Zheng, L.; Jiao, S.; Cao, R.; Liu, Z.-P.; Zhou, H.; Tao, X.; Shang, C.; Yao, H.-B. Amorphous Chloride Solid Electrolytes with High Li-Ion Conductivity for Stable Cycling of All-Solid-State High-Nickel Cathodes. *J. Am. Chem. Soc.* **2023**, *145*, 27774–27787.

(56) Zhang, S.; Zhao, F.; Chen, J.; Fu, J.; Luo, J.; Alahakoon, S. H.; Chang, L.-Y.; Feng, R.; Shakouri, M.; Liang, J.; Zhao, Y.; Li, X.; He, L.; Huang, Y.; Sham, T.-K.; Sun, X. A Family of Oxychloride Amorphous Solid Electrolytes for Long-Cycling All-Solid-State Lithium Batteries. *Nat. Commun.* **2023**, *14*, 3780.

(57) Ishiguro, Y.; Ueno, K.; Nishimura, S.; Iida, G.; Igarashib, Y. $TaCl_5$ -Glassified Ultrafast Lithium Ion-Conductive Halide Electrolytes for High-Performance All-Solid-State Lithium Batteries. *Chem. Lett.* **2023**, *52*, 237–241.

(58) Dai, T.; Wu, S.; Lu, Y.; Yang, Y.; Liu, Y.; Chang, C.; Rong, X.; Xiao, R.; Zhao, J.; Liu, Y.; Wang, W.; Chen, L.; Hu, Y.-S. Inorganic Glass Electrolytes with Polymer-like Viscoelasticity. *Nat. Energy* **2023**, *8*, 1221–1228.

(59) Tanaka, Y.; Ueno, K.; Mizuno, K.; Takeuchi, K.; Asano, T.; Sakai, A. New Oxyhalide Solid Electrolytes with High Lithium Ionic Conductivity >10 mS cm^{-1} for All-Solid-State Batteries. *Angew. Chem. Int. Ed.* **2023**, *62*, e202217581.

(60) Zhang, S.; Zhao, F.; Chang, L.-Y.; Chuang, Y.-C.; Zhang, Z.; Zhu, Y.; Hao, X.; Fu, J.; Chen, J.; Luo, J.; Li, M.; Gao, Y.; Huang, Y.; Sham, T.-K.; Gu, M. D.; Zhang, Y.; King, G.; Sun, X. Amorphous Oxyhalide Matters for Achieving Lithium Superionic Conduction. *J. Am. Chem. Soc.* **2024**, *146*, 2977–2985.

(61) Berhaut, C. L.; Lemordant, D.; Porion, P.; Timperman, L.; Schmidt, G.; Anouti, M. Ionic Association Analysis of LiTDI, LiFSI and $LiPF_6$ in EC/DMC for Better Li-Ion Battery Performances. *RSC Adv.* **2019**, *9*, 4599–4608.

(62) Jun, K.; Lee, B.; L. Kam, R.; Ceder, G. The Nonexistence of a Paddlewheel Effect in Superionic Conductors. *PNAS* **2024**, *121*, e2316493121.

(63) Smith, J. G.; Siegel, D. J. Low-Temperature Paddlewheel Effect in Glassy Solid Electrolytes. *Nat. Commun.* **2020**, *11*, 1483.

(64) Zhang, Z.; Nazar, L. F. Exploiting the Paddle-Wheel Mechanism for the Design of Fast Ion Conductors. *Nat. Rev. Mater.* **2022**, *7*, 389–405.

(65) Tsukasaki, H.; Mori, S.; Morimoto, H.; Hayashi, A.; Tatsumisago, M. Direct Observation of a Non-Crystalline State of Li_2S–P_2S_5 Solid Electrolytes. *Sci. Rep.* **2017**, *7*, 4142.

(66) Hayashi, A.; Minami, K.; Tatsumisago, M. High Lithium Ion Conduction of Sulfide Glass-Based Solid Electrolytes and Their Application to All-Solid-State Batteries. *J. Non-Cryst. Solids* **2009**, *355*, 1919–1923.

(67) Strauss, F.; Lin, J.; Janek, J.; Brezesinski, T. Influence of Synthesis Parameters on Crystallization Behavior and Ionic Conductivity of the Li_4PS_4I Solid Electrolyte. *Sci. Rep.* **2021**, *11*, 14073.

(68) Jodlbauer, A.; Spychala, J.; Hogrefe, K.; Gadermaier, B.; Wilkening, H. M. R. Fast Li Ion Dynamics in Defect-Rich Nanocrystalline Li_4PS_4I—The Effect of Disorder on Activation Energies and Attempt Frequencies. *Chem. Mater.* **2024**, *36*, 1648–1664.

(69) Strauss, F.; Teo, J. H.; Janek, J.; Brezesinski, T. Investigations into the Superionic Glass Phase of Li_4PS_4I for Improving the Stability of High-Loading All-Solid-State Batteries. *Inorg. Chem. Front.* **2020**, *7*, 3953–3960.

(70) Winter, E.; Seipel, P.; Miß, V.; Spannenberger, S.; Roling, B.; Vogel, M. ^{7}Li NMR Studies of Short-Range and Long-Range Lithium Ion Dynamics in a Heat-Treated Lithium Iodide-Doped Lithium Thiophosphate Glass Featuring High Ion Conductivity. *J. Phys. Chem. C* **2020**, *124*, 28614–28622.

(71) Lammert, H.; Kunow, M.; Heuer, A. Complete Identification of Alkali Sites in Ion Conducting Lithium Silicate Glasses: A Computer Study of Ion Dynamics. *Phys. Rev. Lett.* **2003**, *90*, 215901.

(72) Tver'yanovich, Yu. S.; Aleksandrov, V. V.; Murin, I. V.; Nedoshovenko, E. G. Glass-Forming Ability and Cationic Transport in Gallium Containing Chalcohalide Glasses. *J. Non-Cryst. Solids* **1999**, *256–257*, 237–241.

(73) Zhang, X.-H.; Adam, J.-L.; Bureau, B. Chalcogenide Glasses. In *Springer Handbook of Glass*; Musgraves, J. D., Hu, J., Calvez, L., Eds.; Springer International Publishing: Cham, **2019**; pp 525–552.

(74) Tatsumisago, M.; Akamatsu, Y.; Minami, T. Ionic Conductivity of ZrF_4–BaF_2–MX (M = Li, Na; X = F, Cl) Glasses. *Solid State Ionics* **1988**, *31*, 41–47.

(75) Tver'yanovich, Yu. S.; Vlček, M.; Tverjanovich, A. Formation of Complex Structural Units and Structure of Some Chalco-Halide Glasses. *J. Non-Cryst. Solids* **2004**, *333*, 85–89.

(76) Patel, S. V.; Lacivita, V.; Liu, H.; Truong, E.; Jin, Y.; Wang, E.; Miara, L.; Kim, R.; Gwon, H.; Zhang, R.; Hung, I.; Gan, Z.; Jung, S.-K.;, Hu, Y.-Y. Charge-clustering induced fast ion conduction in 2LiX-GaF_3: A strategy for electrolyte design. *Sci. Adv.* **2023**, *9*, eadj9930.

(77) Gupta, S.; Yang, X.; Ceder, G. What Dictates Soft Clay-like Lithium Superionic Conductor Formation from Rigid Salts Mixture. *Nat. Commun.* **2023**, *14*, 6884.

(78) Kim, Y.; Saienga, J.; Martin, S. W. Anomalous Ionic Conductivity Increase in Li_2S + GeS_2 + GeO_2 Glasses. *J. Phys. Chem. B* **2006**, *110*, 16318–16325.

(79) Lin, X.; Zhao, Y.; Wang, C.; Luo, J.; Fu, J.; Xiao, B.; Gao, Y.; Li, W.; Zhang, S.; Xu, J.; Yang, F.; Hao, X.; Duan, H.; Sun, Y.; Guo, J.; Huang, Y.; Sun, X. A Dual Anion Chemistry-Based Superionic Glass Enabling Long-Cycling All-Solid-State Sodium-Ion Batteries. *Angew. Chem. Int. Ed.* **2024**, *63*, e202314181.

(80) Yang, X.; Gupta, S.; Chen, Y.; Sari, D.; Hau, H.-M.; Cai, Z.; Dun, C.; Qi, M.; Ma, L.; Liu, Y.; Urban, J. J.; Ceder, G. Fast Room-Temperature Mg-Ion Conduction in Clay-Like Halide Glassy Electrolytes. *Adv. Energy Mater.* **2024**, *14*, 2400163.

(81) Maier, J. Nanoionics: Ion Transport and Electrochemical Storage in Confined Systems. *Nat. Mater.* **2005**, *4*, 805–815.

(82) Clare, A. G.; Wachtel, P. F.; Musgraves, J. D. Halide Glasses. In *Springer Handbook of Glass*; Musgraves, J. D., Hu, J., Calvez, L., Eds.; Springer International Publishing: Cham, **2019**; pp 595–616.

(83) Ghidiu, M.; Schlem, R.; Zeier W. G. Pyridine Complexes as Tailored Precursors for Rapid Synthesis of Thiophosphate Superionic Conductors. Batter. Supercaps **2021**, *4*, 607–611.

(84) Lim, H.-D.; Yue, X.; Xing, X.; Petrova, V.; Gonzalez, M.; Liu, H.; Liu, P. Designing Solution Chemistries for the Low-Temperature Synthesis of Sulfide-Based Solid Electrolytes. *Journal of Materials Chemistry A* **2018**, *6*, 7370–7374.

(85) Li, X.; Liang, J.; Chen, N.; Luo, J.; Adair, K. R.; Wang, C.; Banis, M. N.; Sham, T.-K.; Zhang, L.; Zhao, S.; Lu, S.; Huang, H.; Li, R.; Sun, X. Water-Mediated Synthesis of a Superionic Halide Solid Electrolyte. *Angew. Chem. Int. Ed.* **2019**, *131*, 16579–16584.

(86) Wang, C.; Liang, J.; Luo, J.; Liu, J.; Li, X.; Zhao, F.; Li, R.; Huang, H.; Zhao, S.; Zhang, L.; Wang, J.; Sun, S. A universal wet-chemistry synthesis of solid-state halide electrolytes for all-solid-state lithium-metal batteries. *Sci. Adv*. **2021**, *7*, eabh1896.

(87) Zhao, R.; Kmiec, S.; Hu, G.; Martin, S. W. Lithium Thiosilicophosphate Glassy Solid Electrolytes Synthesized by High-Energy Ball-Milling and Melt-Quenching: Improved Suppression of Lithium Dendrite Growth by Si Doping. *ACS Appl. Mater. Interfaces* **2020**, *12*, 2327–2337.

(88) Krauskopf, T.; Richter, F. H.; Zeier, W. G.; Janek, J. Physicochemical Concepts of the Lithium Metal Anode in Solid-State Batteries. *Chem. Rev.* **2020**, *120*, 7745–7794.

(89) Maier, J. Ionic Conduction in Space Charge Regions. *Progress in Solid State Chem.* **1995**, *23*, 171–263.

(90) Liang, C. C. Conduction Characteristics of the Lithium Iodide-Aluminum Oxide Solid Electrolytes. *J. Electrochem. Soc.* **1973**, *120*, 1289.

(91) Teo, J. H.; Strauss, F.; Walther, F.; Ma, Y.; Payandeh, S.; Scherer, T.; Bianchini, M.; Janek, J.; Brezesinski, T. The Interplay between (Electro)Chemical and (Chemo)Mechanical Effects in the Cycling Performance of Thiophosphate-Based Solid-State Batteries. *Mater. Futures* **2021**, *1*, 015102.

(92) Wang, S.; Zhang, W.; Chen, X.; Das, D.; Ruess, R.; Gautam, A.; Walther, F.; Ohno, S.; Koerver, R.; Zhang, Q.; Zeier, W. G.; Richter, F. H.; Nan, C.-W.; Janek, J. Influence of Crystallinity of Lithium Thiophosphate Solid Electrolytes on the Performance of Solid-State Batteries. *Adv. Energy Mater.* **2021**, *11*, 2100654.

(93) Kato, A.; Yamamoto, M.; Sakuda, A.; Hayashi, A.; Tatsumisago, M. Mechanical Properties of Li_2S–P_2S_5 Glasses with Lithium Halides and Application in All-Solid-State Batteries. *ACS Appl. Energy Mater.* **2018**, *1*, 1002–1007.

(94) Sakuda, A.; Hayashi, A.; Takigawa, Y.; Higashi, K.; Tatsumisago, M. Evaluation of Elastic Modulus of Li_2S–P_2S_5 Glassy Solid Electrolyte by Ultrasonic Sound Velocity Measurement and Compression Test. *J. Ceram. Soc. Jap.* **2013**, *121*, 946–949.

(95) Kalnaus, S.; Dudney, N. J.; Westover, A. S.; Herbert, E.; Hackney, S. Solid-State Batteries: The Critical Role of Mechanics. *Science* **2023**, *381*, eabg5998.

(96) Garcia-Mendez, R.; Smith, J. G.; Neuefeind, J. C.; Siegel, D. J.; Sakamoto, J.; Correlating Macro and Atomic Structure with Elastic Properties and Ionic Transport of Glassy Li_2S–P_2S_5 (LPS) Solid Electrolyte for Solid-State Li Metal Batteries. *Adv. Energy Mater.* **2020**, *10*, 2000335.

(97) Rosenbach, C.; Walther, F.; Ruhl, J.; Hartmann, M.; Hendriks, T. A.; Ohno, S.; Janek, J.; Zeier, W. G. Visualizing the Chemical Incompatibility of Halide and Sulfide-Based Electrolytes in Solid-State Batteries. *Adv. Energy Mater.* **2023**, *13*, 2203673.

(98) Kwak, H.; Wang, S.; Park, J.; Liu, Y.; Kim, K. T.; Choi, Y.; Mo, Y.; Jung, Y. S. Emerging Halide Superionic Conductors for All-Solid-State Batteries: Design, Synthesis, and Practical Applications. *ACS Energy Lett.* **2022**, *7*, 1776–1805.

(99) Samanta, S.; Bera, S.; Biswas, R. K.; Mondal, S.; Mandal, L.; Banerjee, A. Ionocovalency of the Central Metal Halide Bond-Dependent Chemical Compatibility of Halide Solid Electrolytes with Li_6PS_5Cl. *ACS Energy Lett.* **2024**, *9*, 3683–3693.

(100) Kwak, H.; Kim, J.-S.; Han, D.; Kim, J. S.; Park, J.; Kwon, G.; Bak, S.-M.; Heo, U.; Park, C.; Lee, H.-W.; Nam, K.-W.; Seo, D.-H.; Jung, Y. S. Boosting the

Interfacial Superionic Conduction of Halide Solid Electrolytes for All-Solid-State Batteries. *Nat. Commun.* **2023**, *14*, 2459.

(101) Rudola, A.; Sayers, R.; Wright, C. J.; Barker, J. Opportunities for Moderate-Range Electric Vehicles Using Sustainable Sodium-Ion Batteries. *Nat. Energy* **2023**, *8*, 215–218.

(102) Li, S.; Lin, J.; Schaller, M.; Indris, S.; Zhang, X.; Brezesinski, T.; Nan, C.-W.; Wang, S.; Strauss, F. High-Entropy Lithium Argyrodite Solid Electrolytes Enabling Stable All-Solid-State Batteries. *Angew. Chem. Int. Ed.* **2023**, *62*, e202314155.

(103) Kamaya, N.; Homma, K.; Yamakawa, Y.; Hirayama, M.; Kanno, R.; Yonemura, M.; Kamiyama, T.; Kato, Y.; Hama, S.; Kawamoto, K.; Mitsui, A. A Lithium Superionic Conductor. *Nat. Mater.* **2011**, *10*, 682–686.

(104) Lei, L.; Zhang, L. Recent Advance in High-Pressure Solid-State Metathesis Reactions. *Matter and Radiation at Extremes* **2018**, *3*, 95–103.

(105) Martinolich, A. J.; Neilson, J. R. Toward Reaction-by-Design: Achieving Kinetic Control of Solid State Chemistry with Metathesis. *Chem. Mater.* **2017**, *29*, 479–489.

(106) Liu, Y.; Yu, T.; Xu, S.; Sun, Y.; Li, J.; Xu, X.; Li, H.; Zhang, M.; Tian, J.; Hou, R.; Rao, Y.; Zhou, H.; Guo, S. Magicking an Oxyhalide Interface for 4.8 V-Tolerant High-Nickel Cathodes in All-Solid-State Lithium-Ion Batteries. *Angew. Chem. Int. Ed.* **2024**, *63*, e202403617.

Quotes from the Review that we would like highlighted

(1) Given their large chemical design space, glass-ceramic electrolytes hold great potential for major improvements in ionic conductivity, stability, and mechanical softness.

(2) Tailoring disorder via compositional and/or structural complexity, referring to multiphase compositions and distorted polyanion environments, is key to achieving favorable properties in glass-ceramic electrolytes.

(3) Halide-based glass-ceramics entail the possibility to reduce the lithium fraction while maintaining high ionic conductivity and realizing clay-like softness.

TOC Graphic